PHYSICAL REVIEW C **87**, 035201 (2013)

Faddeev-chiral unitary approach to the K^-d scattering length

T. Mizutani*
Department of Physics, Virginia Polytechnic Institute and State University, Blacksburg, Virginia 24061, USA and Theory Center, Thomas Jefferson National Accelerator Facility, Newport News, Virginia 23606, USA

C. Fayard†
Institut de Physique Nucléaire de Lyon, IN2P3-CNRS, Université Claude Bernard, F-69622 Villeurbanne cedex, France

B. Saghai‡
Institut de Recherche sur les lois Fondamentales de l'Univers, DSM/Irfu, CEA/Saclay, F-91191 Gif-sur-Yvette, France

K. Tsushima§
CSSM, School of Chemistry and Physics, The University of Adelaide, SA 5005, Australia
(Received 25 November 2012; revised manuscript received 26 January 2013; published 5 March 2013)

Our earlier Faddeev three-body study in the K^--deuteron scattering length, A_{K^-d}, is revisited here in light of the recent developments on two fronts: (i) the improved chiral unitary approach to the theoretical description of the coupled $\overline{K}N$ related channels at low energies, and (ii) the new and improved measurement from SIDDHARTA Collaboration of the strong interaction energy shift and width in the lowest K^--hydrogen atomic level. Those two, in combination, have allowed us to produce a reliable two-body input to the three-body calculation. All available low-energy K^-p observables are well reproduced and predictions for the $\overline{K}N$ scattering lengths and amplitudes, $(\pi\Sigma)^\circ$ invariant-mass spectra, as well as for A_{K^-d} are put forward and compared with results from other sources. The findings of the present work are expected to be useful in interpreting the forthcoming data from CLAS, HADES, LEPS, and SIDDHARTA Collaborations.

DOI: 10.1103/PhysRevC.87.035201 PACS number(s): 11.80.Jy, 13.75.Jz

I. INTRODUCTION

There has been a fair amount of recent interest in the low-energy interaction of the $\overline{K}$ with the nucleon, the few nucleon systems, as well as nuclear matter. From the point of view of possible quasibound states, particularly the $\overline{K}NN$, quite a few model discussions have been made during the last decade. Relevant references may be found in Refs. [1–24].

The essential ingredient is, of course, in the two-body $\overline{K}N$ system. From late 1970s, during about two decades, data coming from the kaonic hydrogen atom created significant confusion in this realm, because they were impossible to reconcile with available theoretical approaches (see, e.g., Ref. [25]). Finally in 1997, new data on the strong interaction level shift (ΔE_{1s}) and width (Γ_{1s}) of the K^--hydrogen atomic level became available from KEK [26,27] and were found, for the first time, to be consistent with the low-energy K^-p scattering data. In 2005, a new measurement of ΔE_{1s} and Γ_{1s} became available from the DEAR Collaboration [28], but statistically that appeared to be mutually exclusive with the earlier KEK result. Finally, in 2011 the SIDDHARTA Collaboration released [29] a more precise measurement of ΔE_{1s} and Γ_{1s}. To shed light on the situation with respect to the three sets of data, we recall below the central values and associated total uncertainties $\delta_{\rm tot} = \sqrt{\delta^2_{\rm stat} + \delta^2_{\rm sys}}$,

$$\Delta E_{\rm KEK} = -323 \pm 64 \text{ eV}; \quad \Gamma_{1s}^{\rm KEK} = 470 \pm 231 \text{ eV}, \tag{1}$$

$$\Delta E_{1s}^{\rm DEAR} = -193 \pm 37 \text{ eV}; \quad \Gamma_{1s}^{\rm DEAR} = 249 \pm 115 \text{ eV}, \tag{2}$$

$$\Delta E_{1s}^{\rm SIDD} = -283 \pm 36 \text{ eV}; \quad \Gamma_{1s}^{\rm SIDD} = 541 \pm 92 \text{ eV}. \tag{3}$$

Then, a few comments are in order:

(i) Comparing DEAR and SIDDHARTA data shows almost identical uncertainties on ΔE_{1s} and an improvement of about 20% on Γ_{1s}, however, the discrepancies between the central values come out to be about 2.5σ for both ΔE_{1s} and Γ_{1s}.

(ii) Discrepancies in the central values between KEK and SIDDHARTA data show agreements within 1σ for both ΔE_{1s} and Γ_{1s}.

(iii) SIDDHARTA data improve significantly the precision compared to those reported by KEK, namely, total uncertainties go down from 20% to 13% for ΔE_{1s} and from 49% to 17% for Γ_{1s}.

In spite of ups and downs in experimental results, on the theoretical side, inspired by an earlier work [1], an advanced description of the low-energy coupled $\overline{K}N$ system became available [2], which was based on the nonlinear chiral Lagrangian for the interaction of the octet pseudoscalar mesons and octet baryons; hereafter we refer to this type of approach [30–35] as the Chiral Perturbation Theory (χPT).

New and improved χPT calculations of the coupled $\overline{K}N$ channels observables were then developed [36–41], taking up to the next-to-leading order (NLO) terms in the

*mizutani@vt.edu
†c.fayard@ipnl.in2p3.fr
‡bijan.saghai@cea.fr
§kazuo.tsushima@gmail.com

chiral expansion used in the driving terms of the scattering equation. Borasoy *et al.* [36–38] showed that the inclusion of the DEAR data made some postdicted cross sections deviate significantly from the data. Hereafter the paper by Borasoy, Nissler and Weise [37] is referred to as BNW. Still within another χPT approach [39,41], two types of solution amplitudes were found: one (A_4^+) consistent with the DEAR data, but the other (B_4^+) not. A more recent work [42,43] used a chirally motivated separable model to study the coupled $\overline{K}N$ channels, producing somewhat lower K^-p elastic cross sections compared to the data, and the atomic level width came out to be quite larger in magnitude than the DEAR data, although the latter was used to constrain the fit.

Finally, with regard to works incorporating the SIDDHARTA data, there are two new and improved χPT calculations of the $\overline{K}N$ amplitudes [16,23] (to be discussed later).

During that period, K^-d scattering length was investigated by several authors, though no data are still available. The χPT was exploited [44] to perform a three-body calculation of A_{K^-d}, within the fixed center approximation (FCA) in the input $\overline{K}N$ amplitudes. In the presence of a two-body resonance near threshold [i.e., $\Lambda(1405)$] this approximation had been known to lack accuracy. We performed a relativistic three-body calculation of this quantity [4] that automatically took into account such effects as nucleon binding, target recoil, intermediate nucleon-hyperon interactions, etc. In addition, we demonstrated [3,4] the importance of retaining the deuteron D state, and estimated other possible effects not included in the calculations such as three-particle forces, Coulomb interaction, etc. Our model prediction was $A_{K^-d} = (-1.80 + i1.55)$ fm with an uncertainty of about $\pm 10\%$. Later, a work [45] came out in which an ingenious method was devised in extracting the $\overline{K}^\circ d$ scattering length from the reaction $pp \to \overline{K}^\circ K^+ d$ [46]. The result appeared to prefer a smaller value in magnitude both for the real and imaginary parts: It looked as if our model results were off by two to three standard deviations. However, in view of some assumptions and approximations adopted in Ref. [45] [such as the scattering length approximation to the final state enhancement factor which might well vary rapidly due to the $\Lambda(1405)$], their prediction might be of a semiquantitative nature (we note that the quoted values from our model prediction in that work were incorrect).

During the DEAR era, Meissner *et al.* [47] put forward the ranges of allowed values for scattering lengths $a_{\overline{K}N}$ and A_{K^-d} by making use of the FCA. With the value of a_{K^-p} extracted from the DEAR experiment, almost all the existing model results for A_{K^-d} were shown to stay outside the determined limits. Nevertheless, the corresponding limits on the range extracted from the KEK data happened to be far more accommodating.

At the three-body level, an early work [47] was improved and came up with results [48] less restrictive than with the input from the DEAR data for A_{K^-d}. The inclusion of the recoil effect to FCA [49] is expected to modify the prediction somewhat for the better. In a recent work [50] on A_{K^-d} a standard separable interaction [51] was adopted, but with two-body two-channel ($\overline{K}N - \pi\Sigma$) potentials with a pole [to mimic the $\Lambda(1405)$] fitted to the principal K^-p initiated channels, and the SIDDHARTA data. This is a refinement to a somewhat earlier work by the same author [52]. We note yet another piece of recent work [53] in which the SIDDHARTA result was incorporated in a FCA calculation of A_{K^-d} as well as the corresponding K^--deuteron p-wave scattering volume to predict the p-wave atomic energy shift and width in the K^- deuterium, where two sets of very distinct solutions were reported.

Following recent findings, in the present paper we revisit our previous work [3,4] within an improved χPT for the coupled-channel $\overline{K}N$ amplitudes, using them to obtain A_{K^-d}.

The organization of the present paper is as follows: Section II describes the χPT approach to the coupled $\overline{K}N$ channels, which is the primary input to our calculation of A_{K^-d}; Sec. III A embodies a brief description of the three-body calculation we have adopted [4]. The numerical method is outlined in Sec. III B and our results reported and discussed in Sec. III C. Finally, Sec. IV serves to draw our conclusions. We relegate to Appendix some of the useful formulas for Sec. II.

II. TWO-BODY CHANNELS

Because the nucleon-nucleon (NN) two-body interaction that we have adopted in the present work is the same as that used in Refs. [3,4], this section is devoted to the coupled $\overline{K}N$ channel interactions that are the primary two-body ingredient to the three-body approach.

For the two-body $\overline{K}N$ channels, we adopted a chiral interaction Lagrangian which contains the meson $\phi \equiv (\pi, K, \eta)$ and baryon $B \equiv N, \Lambda, \Sigma, \Xi$ fields, as reported below.

A. $\overline{K}N$ interactions

Coupled-channel equations determine the reaction among various two-body meson-baryon channels. For our present study these are $\overline{K}N$, πY, ηY, and $K\Xi$ with different charge states. By using $i,\ j,\ k, \ldots$, as channel indices, the coupled Bethe-Salpeter equations for the t matrices for the scattering process $i \to j$ reads

$$T_{ij} = V_{ij} + \sum_k V_{ik} G_0^k T_{kj}, \tag{4}$$

where V_{ij} is the transition potential (or the driving term) taken from an effective chiral Lagrangian to be discussed below, and G_0^k is the free meson-baryon propagator for the intermediate channel k. We note here that implicit in the above expression are that (i) although not essential, the meson-baryon systems are in the two-body center-of-mass (c.m.) frame, and (ii) the integration is performed over the off-shell four-momentum associated with channel k. It is also possible to write the above set of equations collectively in a simple matrix form,

$$\widetilde{T} = \widetilde{V} + \widetilde{V}\widetilde{G}\widetilde{T}, \tag{5}$$

where $\widetilde{V} = \{V_{ij}\}$ is the matrix of driving terms, and similarly for $\widetilde{T}$, while $\widetilde{G}$ is a diagonal matrix with elements G_0^k in the diagonal.

Next, in a standard χPT approach one makes an *on-shell* ansatz [2] in which both $\widetilde{V}$ and $\widetilde{T}$ are put fully *on-shell* with respect to the initial c.m. channel energy, $W \equiv \sqrt{s}$, with s being the Mandelstam s variable for all the channels involved.

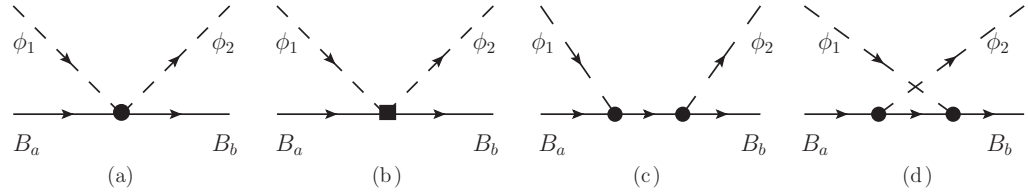

FIG. 1. Diagrams for meson-baryon scattering: seagull or the Weinberg-Tomozawa interaction (a), contact interactions or the next-to-leading order (b), direct s-channel (c), and crossed u-channel Born terms. Dashed and solid lines are for mesons and baryons, respectively.

Then this ansatz renders the above equation into an algebraic one for which the solution becomes

$$\widetilde{T} = [1 - \widetilde{V}\widetilde{G}(s)]^{-1}\widetilde{V}, \tag{6}$$

where the diagonal elements of $\widetilde{G}(s)$ are now the *off-shell momentum* integrated G_0^k(s), often called *scalar loops* and are functions of only s. Note that our sign convention for $\widetilde{V}$ and $\widetilde{T}$ is the opposite of the one adopted in Refs. [36,37]. A more detailed account is given in Appendix.

Now we need to specify the fully on-shell $\widetilde{V}$ (or V_{ij}). As has become standard by now, one obtains these driving terms from a Lagrangian with nonlinear realization of chiral symmetry. We refer the reader to Refs. [36,37] whose notation and description we will closely follow in our subsequent description.

Four terms from two primary sources are included for $\widetilde{V}$, Fig. 1, as follows:

(i) The leading order contact term in the Lagrangian providing the commonly called Weinberg-Tomozawa (WT) leading order contact term $\widetilde{V}^{(a)}$, two Born terms: direct s-channel $\widetilde{V}^{(c)}$ and crossed u-channel $\widetilde{V}^{(d)}$, which contain two axial vector coupling constants D and F. As in BNW, we have adopted the frequently used central values [54], namely, $D = 0.80$ and $F = 0.46$, subject to constraint by the nucleon axial-vector coupling constant in the chiral limit, i.e., $D + F = g_A = 1.26$.

(ii) The NLO term $\widetilde{V}^{(b)}$ is of the second chiral order $\mathcal{O}(p^2)$, and contains a chiral symmetry breaking measure (B_0) arising from the chiral condensate, as well as u, d, and s current quark masses. The dependence on those quantities is eventually converted to that on the physical meson masses, using the Gell-Mann-Oakes-Renner relation for the Goldstone boson masses. In addition, for our current objective, this part of the interaction depends on seven *low-energy constants* [1]: b_0, b_D, b_F, d_1, d_2, d_3, and d_4, which should be determined from fits to relevant physical observables. As for the first three parameters which are determined from our present fit to available low-energy cross sections, we will call them the *renormalized b* parameters: $\bar{b}_0$, $\bar{b}_D$, and $\bar{b}_F$. The reason for this may be found in Refs. [16,17], and in our later discussion. For convenience, we also introduce different combinations of driving terms, called the WT, c, s, and u models as follows:

$$\begin{aligned} \widetilde{V}_{WT} &\equiv \widetilde{V}^{(a)}, \quad \widetilde{V}_c \equiv \widetilde{V}^{(a)} + \widetilde{V}^{(b)}, \\ \widetilde{V}_s &\equiv \widetilde{V}^{(a)} + \widetilde{V}^{(b)} + \widetilde{V}^{(c)}, \\ \widetilde{V}_u &\equiv \widetilde{V}^{(a)} + \widetilde{V}^{(b)} + \widetilde{V}^{(c)} + \widetilde{V}^{(d)}, \end{aligned} \tag{7}$$

so, for example, the s model contains WT, NLO, and s-pole terms.

For the present three-body study with total strangeness of the input meson-baryon system $S = -1$, we need two separate sets of coupled channels among various two-body physical particle states:

$$\begin{aligned} K^- p \to\ & K^- p, \overline{K}^\circ n, \Lambda\pi^\circ, \Sigma^+\pi^-, \Sigma^\circ\pi^\circ, \Sigma^-\pi^+, \\ & \Lambda\eta, \Sigma^\circ\eta, [K^+\Xi^-], [K^\circ\Xi^\circ], \end{aligned} \tag{8}$$

$$K^- n \to K^- n, \Lambda\pi^-, \Sigma^\circ\pi^-, \Sigma^-\pi^\circ, \Sigma^-\eta, [K^\circ\Xi^-]. \tag{9}$$

The first set contains 10 channels ($N_{K^-p} = 10$) and the second one six ($N_{K^-n} = 6$). Thus for the first set, Eq. (8), channels indices i, j for V_{ij} run from 1 to 10. We note that the square bracketed channels in the two equations above were *not* included in our 2002/2003 works [3,4] although most of the later works have retained them conventionally. As explained later, in the present study we began with the $[N_{K^-p} = 10, N_{K^-n} = 6]$ scheme, then based on the statistical fit to data, eventually went back to the earlier choice of $[N_{K^-p} = 8, N_{K^-n} = 5]$.

Having specified the channels, the concrete form of the driving term may now be identified; Refs. [17,37] provide all the necessary information; see also Sec. III 3 of Ref. [24] (note the difference in the overall sign and in spinor normalization in these references). These driving terms may need to be spin averaged and projected onto the s-wave orbital state before fed into the scattering equation. In these expressions of the driving terms, the weak decay constant f enters everywhere. Recall that due to the on-shell ansatz [2], its value is expected to be different either from the one in the chiral limit, or the physical ones for pion, kaon, or η decays. For our objective its value is determined by fits to the scattering data whereas in recent works [16,17] f_π was fixed at the physical value and f_K, f_η were floated around their physical values and determined by fits.

Once the driving terms are specified, the last quantity we need to take care of, before performing statistical fits to determine the scattering t matrix $\widetilde{T}$, is $\widetilde{G}(s)$ whose j^{th} diagonal matrix element is a scalar loop,

$$G^j(s) = \int \frac{d^4q}{(2\pi)^4} \frac{i}{\left[(p-q)^2 - M_j^2 + i\epsilon\right]\left[q^2 - m_j^2 + i\epsilon\right]}, \tag{10}$$

where $p^2 = s$ and M_j (m_j) are the baryon (meson) masses in the j^{th} channel. This is a divergent integral, made finite by dimensional regularization which introduces subtraction constants a_j, $j = 1, 2, \ldots$. These constants are also to be

fixed by fits to the scattering data. Because a scalar loop is characterized only by masses of the particles involved, assuming isospin symmetry to reduce the number of these subtraction constants may be quite relevant, so for the number of channels $N_{K^-p} = 10\,(8)$ the number of a_js is 6 (5). For more on the scalar loops, see Appendix. Here it should be useful to mention a very recent work [23], which is within the χPT, but without the on-shell ansatz. Furthermore, (i) it corresponds to the c model mentioned above, but included more NLO terms (see the reason behind this choice in Ref. [55]), (ii) only the first six channels ($N_{K^-p} = 6$) are included in the fitting procedure that are open in the energy range for the adopted data.

Before proceeding to the determination of $\widetilde{T}$ using statistical fits to data, it should be useful to discuss a couple of items.

First, we need to state where the present work is different from our 2002/2003 study [3,4].

(i) Our earlier work [4] included only the WT interaction $\widetilde{V}_{WT}$ in the driving term whereas in the present work we go further to include the NLO contribution, so the c model $\widetilde{V}_c$, and also the s model $\widetilde{V}_s$. In practice we have excluded the u model $\widetilde{V}_u$ for reasons to be stated soon below. Note that the form of the WT interaction used then and in the present work are equivalent except for a small contribution disregarded in the former.

(ii) Our earlier work introduced a global form factor in the driving terms to tame the *otherwise divergent* integral for loop functions. We feel that the dimensional regularization in the present work is more consistent in spirit with respecting chiral symmetry.

(iii) Apart from physical masses, the implementation of the SU(3) symmetry breaking was in the different values of the meson decay constant in our previous work, but in the values of the subtraction constants in the present study.

The second item is on the interaction models we have chosen in the present study as just stated in (i) above. As mentioned in BNW, upon adopting the on-shell ansatz, and upon projecting onto the s ($l = 0$) orbital angular momentum state, the u-pole contribution $\widetilde{V}^{(d)}$ develops logarithmic dependence on the Mandelstam variable s. This type of logarithmic dependence is generally mild and the resultant interaction of lesser importance relative to other contributions, except that the branch cuts from the higher threshold channels extend up to the threshold of some light meson-baryon channels. We should stress that those branch cuts are *unphysical* originating from the on-shell ansatz. Possible cures may be (a) as in BNW, to eliminate the singularities by matching the amplitude appropriately to some constant where relevant, (b) no particular modification to eliminate the branch cuts by arguing that they might only affect a less dominant amplitude for elastic $\pi^\circ\Lambda$ below the $\pi\Sigma$ threshold [40], or (c) to adopt a static approximation to baryons in the u-pole terms as done, for example, in [43].

Here in our work, we simply do not include the u-pole contributions in the driving term by acknowledging their relatively weak contribution as already stated above. Thus we have studied just the c and s models. Underlining this is the observation that, as may be easy to understand from the static limit, the s- and u-pole terms tend to compensate each other. Consequently, a *properly regulated* u model is expected to provide resultant amplitudes and observables which may well come out somewhere between the corresponding quantities from the c and s models. We should emphasize here that once the coupled two-body $\overline{K}N$ amplitudes are fed into the coupled three-body equations, the loop momentum integrations go down below the threshold of those two-body amplitudes, so it is essential that the result of the three-body calculation not be distorted by any unwanted singularities, hence our choice above! Because only BNW have presented separately the cases with c- and s-models' results, we were compelled to construct our own $\overline{K}N$ channel amplitudes.

To be complete, in Table I we list the physical particle masses [56] used in the present work.

B. Data base and extraction of adjustable parameters

Here, we report on the data used to extract the adjustable parameters for our two-body amplitudes.

In the energy range of interest in this work ($P_{K^-} \lesssim 250$ MeV/c), total cross-section measurements were performed between the 1960s and 1980s, producing [57–66] some 90 data points for the following channels: $K^-p \to K^-p$, $\overline{K}^\circ n$, $\Lambda\pi^\circ$, $\Sigma^+\pi^-$, $\Sigma^\circ\pi^\circ$, and $\Sigma^-\pi^+$. Given that the complete data set shows internal inconsistencies, reduced sets are used in various fitting procedures and the number of retained data points is not identical in reported phenomenological investigations. Here, we have adopted the same approach as in Refs. [3,4,67], where 52 cross-section data [58,59,62,63,65] were selected. The method used there was to fit all 90 cross-section data, as well as the accurate data [59,60,68–70] for K^-p reaction rates at threshold, i.e.,

$$\gamma = \frac{K^-p \to \pi^+\Sigma^-}{K^-p \to \pi^-\Sigma^+} = 2.36 \pm 0.04, \tag{11}$$

$$R_c = \frac{K^-p \to \text{charged particles}}{K^-p \to \text{all final states}} = 0.664 \pm 0.011, \tag{12}$$

$$R_n = \frac{K^-p \to \pi^\circ\Lambda}{K^-p \to \text{all neutral states}} = 0.189 \pm 0.015. \tag{13}$$

Then, cross-section data giving the highest χ^2 were removed and the reduced data base was refitted. Checking

TABLE I. Particle masses (in MeV).

K^-	K^+	$\overline{K}^\circ$	p	n	π^-	π^+	π°	Σ^-	Σ^+	Σ°	Λ	η	Ξ^-	Ξ°
493.68	493.68	497.65	938.27	939.57	139.57	139.57	134.98	1197.45	1189.37	1192.64	1115.68	547.51	1321.31	1314.83

TABLE II. Adjustable parameters in the present work. The weak decay constant f is in MeV. The renormalized NLO parameters ($\bar{b}_0$, $\bar{b}_D$, $\bar{b}_F$) and the low-energy constants in the NLO Lagrangian (d_1, d_2, d_3, d_4) are in GeV^{-1}. The subtraction constants $a(\mu)$ are given at $\mu = 1$ GeV.

Parameter	Model c	Model s
f	116.2 ± 0.7	122.4 ± 0.9
$\bar{b}_0$	-0.35 ± 0.01	-0.40 ± 0.02
$\bar{b}_D$	0.01 ± 0.02	-0.08 ± 0.01
$\bar{b}_F$	-0.02 ± 0.02	-0.04 ± 0.03
d_1	-0.17 ± 0.02	-0.11 ± 0.03
d_2	0.07 ± 0.01	0.06 ± 0.01
d_3	0.29 ± 0.01	0.26 ± 0.02
d_4	-0.34 ± 0.01	-0.28 ± 0.02
$a_{\overline{K}N}$ ($\times 10^{-3}$)	1.60 ± 0.08	1.89 ± 0.10
$a_{\pi\Lambda}$ ($\times 10^{-3}$)	-8.59 ± 2.33	0.96 ± 3.29
$a_{\pi\Sigma}$ ($\times 10^{-3}$)	1.15 ± 0.33	-0.05 ± 0.34
$a_{\eta\Lambda}$ ($\times 10^{-3}$)	-2.30 ± 0.26	-1.86 ± 0.34
$a_{\eta\Sigma}$ ($\times 10^{-3}$)	2.99 ± 3.91	-6.35 ± 4.90
$\chi^2_{d.o.f.}$	1.22	1.21

the outcome of several combinations of data sets allowed establishing a consistent enough data base. In the present work, in addition, the strong interaction level shift (ΔE_{1s}) and width (Γ_{1s}) of the K^--hydrogen atomic level data from the SIDDHARTA Collaboration [29] were also included in the data base, without affecting the acceptable consistency of the kept total cross-section data. Finally, we added to the data base the pion-nucleon sigma term, $\sigma_{\pi N} = 35 \pm 10$ MeV, which brings in a loose constraint (we will come back to this issue at the end of this section). In summary, our data base embodies a total of 58 data points.

Our approach for $N_{K^-p} = 8$ contains 13 adjustable parameters, as reported in Table II.

The uncertainties attributed to our results are those generated by MINUIT, used for minimizations. Our c and s models lead both to $\chi^2_{d.o.f.} \approx 1.2$. As much as the subtraction constants are concerned, taking into account the uncertainties, we observe that $a_{\pi\Lambda}$, $a_{\pi\Sigma}$ and $a_{\eta\Sigma}$ are somewhat poorly determined.

Here, we discuss some issues related to the pion-nucleon sigma term $\sigma_{\pi N}$. While we want to perform our fit by using direct experimental data only, we are interested in the extent to which the constraint from the pion-nucleon sigma term may affect the resulting data fit. At leading order the sigma term reads

$$\sigma^0_{\pi N} = -2m_\pi^2(2b_0 + b_D + b_F). \tag{14}$$

It is well known that the pion-nucleon σ term, obtained by Gasser *et al.* [71], based on πN data analysis and taking into account the current algebra result generated by the quark masses, gave $\sigma_{\pi N} = 45 \pm 8$ MeV. More recent investigations lead either to smaller or larger values with respect to the central one, 45 MeV. For instance, (i) a pertubative chiral constituent quark model [72] finds 55 MeV, an analysis of πN scattering amplitude via chiral perturbation theory [73] reaches 59 ± 7 MeV, or still a dispersion relations approach [74], using the SAID πN phase-shift analysis [75] gives $\sigma_{\pi N} = 81 \pm 6$ MeV; (ii) on the other hand, lattice QCD calculations lead to 39 ± 4 MeV [76], 38 ± 12 MeV [77], 45 ± 6 MeV [78], while chiral constituent quark models [79] predict 31 MeV [80] or 37 MeV [81].

In recent works [39,41–43], including the present one, some of the NLO low-energy constants (notably $\bar{b}_0$, $\bar{b}_D$, and $\bar{b}_F$) are constrained by using the lowest order terms for meson and/or baryon mass formula (Gell-Mann-Okubo mass formula), as well as the pion-nucleon sigma term $\sigma_{\pi N}$ within the context of the chiral perturbation theory (χPT).

On the other hand, by calculating the corresponding value from several χPTs for the coupled $\overline{K}N$ system [17,37,38], one finds lower values of $\sigma_{\pi N} \approx 15$–$30$ MeV. However, as discussed briefly in Ref. [17], the latter is the result of the fit to scattering data by iterating the driving term (with physical hadron masses adopted) which contains those NLO constants to infinite orders. The extracted values of these constants are then expected to be different from those obtained by fitting baryon masses perturbatively; see, e.g. Ref. [17]. So as stated earlier, we denote the former set of the corresponding values as $\bar{b}_0$, $\bar{b}_D$, $\bar{b}_F$, and the corresponding sigma term as $\bar{\sigma}^{(0)}_{\pi N}$, as in Ref. [17].

In the present work, performing minimizations with no constraint on the sigma term, $\bar{\sigma}^{(0)}_{\pi N}$ was found to fluctuate around $15 \sim 20$ MeV. Trying to enforce the sigma term in the region 50–85 MeV resulted in clustering near the lowest limit. While letting that term vary in the range 25–45 MeV, the minimization went smoother, with little effect on the χ^2. So with the loose constraint $25 \leqslant \bar{\sigma}^{(0)}_{\pi N} \leqslant 45$ MeV, we performed the final minimizations. The parameters reported in Table II lead to $\bar{\sigma}^0_{\pi N} = 28$ MeV and 36 MeV for models c and s, respectively.

To end this section, we would like to comment about other channels, $K^-p \to \eta\Lambda$, $K\Xi$, with thresholds beyond the energy range investigated in this work.

With $N_{K^-p} = 10$ fit, the last subtraction constant $a_{K\Xi}$ tends to get quite large relative to others, with sizable uncertainty. This indicates that the two $K\Xi$ channels are very likely not relevant to the low-energy fit, and the extracted $a_{K\Xi}$s have no actual substance. To test this observation from several $N_{K^-p} = 10$ fits, we dropped the last two $K\Xi$ channels in Eq. (8), and ran the effective $N_{K^-p} = 10 - 2 = 8$ channel models to calculate the corresponding observables. The result was found just about $\sim$5% different from the original $N_{K^-p} = 10$ cases. To confirm this, we also used $N_{K^-p} = 8$ fit results, then added two extra $K\Xi$ channels from a few $N_{K^-p} = 10$ fit results, to make an effective $N = 8 + 2 = 10$ model. Again, the latter was found to reproduce the observables calculated in $N_{K^-p} = 8$ configuration within $\sim$5%. Also with respect to the data set used in the present work, the $N_{K^-p} = 8$ minimizations are slightly better than the ones with $N_{K^-p} = 10$ in $\chi^2_{d.o.f.}$ by about 0.1. So we felt justified to adhere to the $N_{K^-p} = 8$ model. Therein, we kept $K^-p \to \eta Y$ channels which have lower thresholds compared to $K\Xi$ final states, but because of lack of low-energy data, we could only check the smooth rising of the cross section close to threshold, matching the lowest energy $K^-p \to \eta\Lambda$ data points reported by the Crystal Ball Collaboration [82]. Finally, recent studies at higher energies

can be found, e.g., in [82,83] for $\eta\Lambda$ final state and in Refs. [41,84,85] for $K\Xi$ final states.

C. Results and discussion

In this section we present our results and compare them with the data, namely, cross sections for K^-p initiated reactions, threshold strong channel branching ratios, and kaonic hydrogen atom $1s$ level shift. Then we will report on our predictions for the scattering lengths and amplitudes, as well as for the $(\pi\Sigma)^\circ$ invariant-mass spectra.

1. Total cross sections

In the low-energy range of our current interest, i.e., $P_K^{\rm lab} \leqslant 250$ MeV/c, the following strong coupled channels are open:

$$K^-p \to K^-p, \overline{K}^\circ n, \Lambda\pi^\circ, \Sigma^+\pi^-, \Sigma^\circ\pi^\circ, \Sigma^-\pi^+, \quad (15)$$

and strongly influenced by the $I = 0\,\Lambda(1405)$ resonance below the K^-p threshold which decays almost exclusively to $\pi\Sigma$. Moreover, while the $\overline{K}^\circ n$ has a slightly higher threshold, all the πY channels have lower threshold than that for K^-p.

Our c-model results for all open strong channels are reported in Fig. 2 and compared to the data. The s model gives very close values to those of the c model, so they are not depicted.

As mentioned above, we have retained 52 data points for those channels. The obtained χ^2 per data point ($\chi^2_{d.p.}$) turns out to be 0.98. Our model allows reproducing the total cross section data satisfactorily. This is also the case for the BNW model, also for the c model (close to the s one). The only discrepancy between the two models concerns the $\overline{K}^\circ n$ final state, due to the respective fitted data bases.

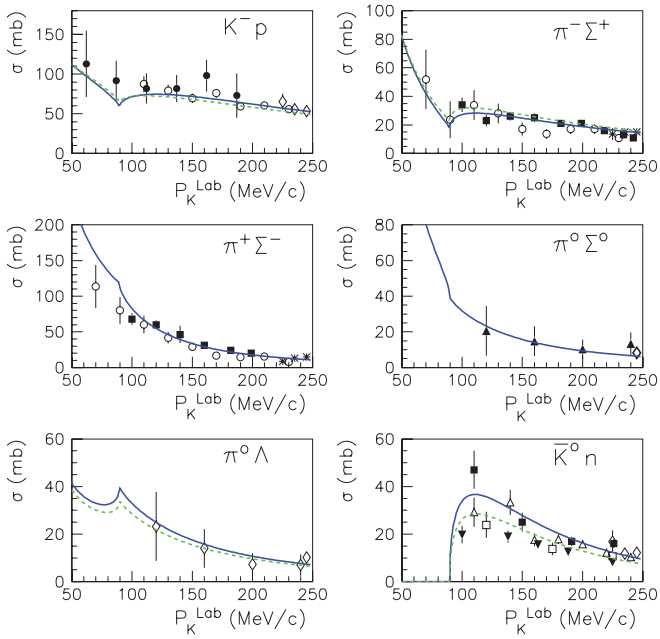

FIG. 2. (Color online) Total cross sections initiated by K^-p. The solid (blue) curves are our fits and the dashed (green) lines our results for the BNW model [37]; both sets are given for the c model. The solid and dashed curves are almost identical for $\pi^+\Sigma^-$ and $\pi^\circ\Sigma^\circ$. Experimental data are from Refs. [58,59,62,63,65].

2. Threshold strong branching ratios and kaonic atom

Table III summarizes theoretical and experimental values for K^-p reaction rates: γ, R_c, and R_n [Eqs. (11)–(13)], as well as K^--hydrogen atomic $1s$ level shift and width. We get $\chi^2_{d.p.} = 0.99$ for the branching ratios and $\chi^2_{d.p.} = 0.21$ for the SIDDHARTA kaonic hydrogen atom data.

Our c- and s-model results are close to each other and they agree with the data within less than 1σ. Results from other calculations, briefly presented in previous sections, show similar trends. We will come back to those works in the following section.

It is worth recalling that the work by Borasoy *et al.* [37] (BNW) was published before the SIDDHARTA data release.

The only significant deviation from data concerns the width Γ_{1s} reported in a very recent work [87], based on the first-order Lagrangian, solving the Lippmann-Schwinger equation with separable interaction potential.

3. Scattering lengths

In view of the K^-d scattering length investigations, in addition to K^-p initiated processes, Eq. (8), we need to determine amplitudes for the reactions having as initial state K^-n, Eq. (9), for which there are no data. The adopted procedure is then as follows: Once the parameters for the T matrices for the K^-p channels, Eq. (8), are determined by fit to the data, they are used to calculate the T matrices for the K^-n channels, Eq. (9), by assuming SU(3) symmetry in the coupling strengths. Those two sets of amplitudes are then used in the three-body calculation of A_{K^-d}.

Here along with the corresponding quantity in the K^-p initiated channels, we present the scattering lengths as given in Table IV. For "Data", kaonic atom measurements are used to extract the scattering lengths. "Data" for KEK and DEAR are from Weise [88]. For SIDDHARTA, we used the improved [89] Deser-Trueman formula to relate the measured quantities to the complex $K^-p \to K^-p$ scattering length,

$$\Delta E_{1s} + \tfrac{1}{2}i\Gamma_{1s} = 2\alpha^3\mu^2 a_{K^-p}[1 - 2\alpha\mu(ln\alpha - 1)a_{K^-p}], \quad (16)$$

with α the fine-structure constant and μ the K^--proton reduced mass.

Note that the scattering lengths in Table IV have been obtained at the K^-p threshold (except for the elastic K^-n process). In fact, these quantities are very sensitive to the value of the threshold at which they are calculated, which is then reflected in the values obtained for the A_{K^-d} scattering length. These aspects have been discussed in a previous paper [4].

The scattering lengths, Table IV, show several features as summarized in the following: (i) Both real and imaginary parts of a_p agree with data within 1σ for all models, with the only exception being BNW model c produced before the release of SIDDHARTA data; (ii) for the three other scattering lengths, models' predictions for the imaginary parts, as well as for $\mathcal{R}e(a_{ex})$ are compatible with each other; (iii) finally,

TABLE III. The $K^- p$ threshold strong branching ratios, kaonic atom $1s$ level shift, and width (in eV). See text for experimental data references. Results for BNW models were obtained using their parameters in our code.

Authors [Ref.]	γ	R_c	R_n	$-\Delta E_{1s}$	Γ_{1s}
Present work (c)	2.36	0.646	0.190	314	589
Borasoy *et al.* [37] [BNW (c)]	2.36	0.655	0.191	316	562
Present work (s)	2.40	0.645	0.189	304	591
Borasoy *et al.* [37] [BNW (s)]	2.27	0.652	0.192	350	535
Mai-Meissner [23] (c-type model)	2.44 ± 0.70	0.643 ± 0.017	0.268 ± 0.098	296 ± 52	600 ± 49
Ikeda, Hyodo, Weise [17] (u model)	2.37	0.66	0.19	306	591
Shevchenko [50] (one-pole)				313	597
Shevchenko [50] (two-pole)				308	602
Cieply-Smejkal [86] (NLO)	2.37	0.660	0.191	310	607
Krejcirik [87]	2.36	0.637	0.178	296	761
Experiment	2.36 ± 0.04	0.664 ± 0.011	0.189 ± 0.015	283 ± 36	541 ± 92

in the case of $\mathcal{R}e(a_n)$ and $\mathcal{R}e(a_n^\circ)$, our predictions turn out to be significantly larger than results from other findings. The sensitivity of scattering lengths to model ingredients, especially to the NLO contributions, are discussed in Ref. [17].

4. Scattering amplitudes

It is instructive to investigate the real and imaginary parts of the $\overline{K}N$ scattering amplitudes below threshold: $\sqrt{s} \approx 1.432$ GeV for $K^- p$, 1.433 GeV for $K^- n$, and 1.437 GeV for $\overline{K}^\circ n$.

Figures 3 and 4 show the amplitudes (f) for elastic scattering channels, obtained from our model c, as well as those from BNW. An interesting feature is that for $K^- p \to K^- p$ both the real and imaginary parts of the scattering amplitudes are very close, as predicted by the two depicted models. This, however, is not the case for the $K^- n \to K^- n$ process, where the real part from our model turns out to be significantly larger than the one in BNW, which used DEAR data.

A behavior common to both models is that the maximum of $\mathrm{Im}(f_{K^- p \to K^- p})$ is located at $\sqrt{s} \approx 1.416$ GeV, so in between the $\Lambda(1405)$ and $\sqrt{s_{K^- p}} \approx 1.432$ GeV.

DEAR data were also used in Refs. [43,90,91]. A chiral SU(3) coupled-channel dynamics by Hyodo and Weise [90], embodying only the dominant $\overline{K}p - \pi\Sigma$ channels, led to (much) larger amplitudes, in terms of absolute values. In a separable meson-baryon approach, Cieply and Smejkal [43], using a two-pole configuration, reported larger real part, but comparable imaginary part, though with the maximum around 1.4 GeV. In a recent work based on a coupled-channels Bethe-Salpeter approach, Mai and Meissner [23] investigated the two-pole structure and found somewhat narrow spectrum.

For the $K^- n \to K^- n$ scattering amplitudes there are fewer predictions available. In addition to that by BNW, shown in Fig. 4, Cieply and Smejkal [43] have reported amplitudes with $\mathrm{Re}(f_{K^- n \to K^- n})$ roughly 50% larger than our values and $\mathrm{Im}(f_{K^- n \to K^- n})$ comparable to our results, but with a narrower structure.

5. $\pi\Sigma$ invariant-mass observable

The $(\pi\Sigma)^\circ$ invariant-mass spectra data were not fitted in the present work. So, in Fig. 5 we compare our prediction (full curve) to the $\pi^- \Sigma^+$ data [92] going back to the early 1980s, measured at CERN in the $K^- p \to \Sigma^+ \pi^- \pi^+ \pi^-$ reaction at $P_K = 4.2$ GeV/c; the agreement is reasonable.

Given that the $\Lambda(1405)$ formation, decaying to $\pi\Sigma$, is about 30 MeV below $K^- p$ threshold, a reliable extrapolation

TABLE IV. $\overline{K}N$ scattering lengths (in fm); a_p, a_n°, and a_{ex} are calculated at $W = M_{K^-} + M_p$ and a_n at $W = M_{K^-} + M_n$. See text for "Data" explanation.

Model	$a_p(K^- p \to K^- p)$	$a_n(K^- n \to K^- n)$	$a_n^\circ(\overline{K}^\circ n \to \overline{K}^\circ n)$	$a_{ex}(K^- p \to \overline{K}^\circ n)$
Present work (c)	$-0.72 + i0.90$	$0.86 + i0.71$	$-0.12 + i0.90$	$-1.21 + i0.37$
Borasoy *et al.* [37], BNW (c)	$-0.74 + i0.86$	$0.61 + i0.71$	$-0.24 + i0.96$	$-1.09 + i0.34$
Present work (s)	$-0.69 + i0.89$	$0.90 + i0.66$	$-0.10 + i0.87$	$-1.21 + i0.38$
Borasoy *et al.* [37], BNW (s)	$-0.85 + i0.86$	$0.49 + i0.67$	$-0.38 + i1.01$	$-1.11 + i0.36$
Ikeda *et al.* [17] (u model)	$-0.70 + i0.89$	$0.57 + i0.73$		
Mai-Meissner [23] (c-type model)	$(-0.68 \pm 0.15) + i(0.90 \pm 0.13)$			
Shevchenko [50] (one-pole)	$-0.76 + i0.89$			
Shevchenko [50] (two-pole)	$-0.74 + i0.90$			
"Data":				
SIDDHARTA	$(-0.66 \pm 0.07) + i(0.81 \pm 0.15)$			
KEK	$(-0.78 \pm 0.18) + i(0.49 \pm 0.37)$			
DEAR	$(-0.47 \pm 0.10) + i(0.30 \pm 0.17)$			

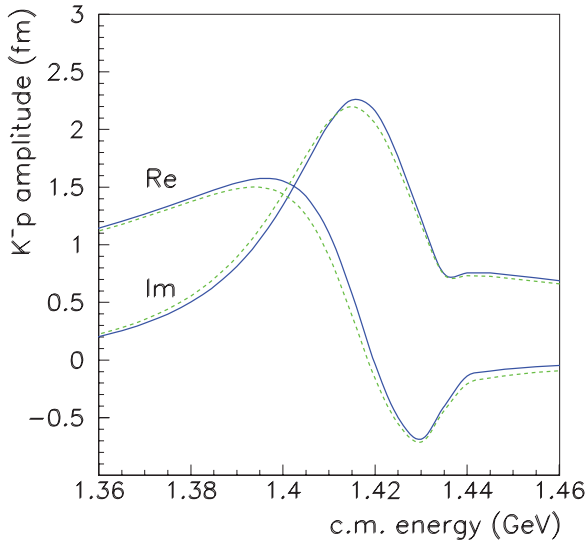

FIG. 3. (Color online) Scattering amplitudes for the $K^- p$ channel within model c with real and imaginary parts from the present work (blue solid curves) with $N_{K^- p} = 8$, and BNW [37] (green dotted curves) with $N_{K^- p} = 10$, obtained using our code.

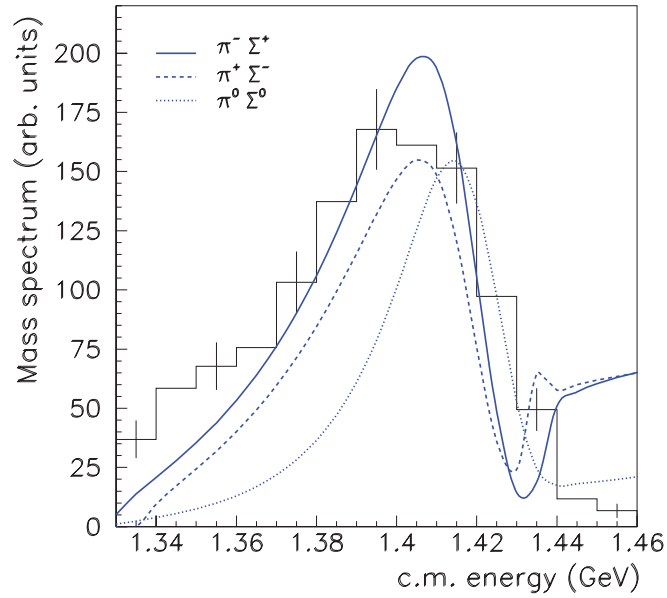

FIG. 5. (Color online) $(\pi\Sigma)^\circ$ invariant mass spectra for $K^- p \to \pi^- \Sigma^+, \pi^+ \Sigma^-, \pi^\circ \Sigma^\circ$ as a function of the total center-of-mass energy.

of $\overline{K}N \to \pi\Sigma$ requires data on the shape and location of the invariant mass spectra for the $\pi^-\Sigma^+$, $\pi^+\Sigma^-$, and $\pi^\circ\Sigma^\circ$ channels, for which our predictions are depicted in Fig. 5 in full, dashed, and dotted curves, respectively. Predictions for all three channels were also reported within chiral approaches [93,94]. It is worth noting that those results endorse our predictions, namely, (i) the magnitude of the $\pi^-\Sigma^+$ peak is higher than those of the other channels, which turn out to have comparable strengths; (ii) the peak of the $\pi^-\Sigma^+$ channel is located at lower energy than those of the two other charge states.

A recent measurement of the $\pi^\circ\Sigma^\circ$ was performed by the ANKE Collaboration [95] for $P^{\rm lab} = 3.65$ GeV/c via the process $pp \to pK^+\pi^\circ\Sigma^\circ$ with somewhat large uncertainties, as discussed in [96], and successfully reproduced within a dynamical chiral SU(3) calculation [97]. Very recently, HADES collaboration released data [98,99] for $pp \to \pi^\pm\Sigma^\mp K^+ p$ at $E^{\rm lab}_{\rm kin} = 3.5$ GeV, and $\Lambda(1405) \to \pi^\pm\Sigma^\mp$ channels were extracted. To that purpose, and to subtract contributions from $pp \to \Sigma^\circ(1385)K^+ p \to \pi^\pm\Sigma^\mp K^+ p$, the experimentally determined [100] cross-section ratio $\sigma_{pp\to\Sigma^\circ(1385)K^+p}/\sigma_{pp\to\Lambda(1405)K^+p}$ was used.

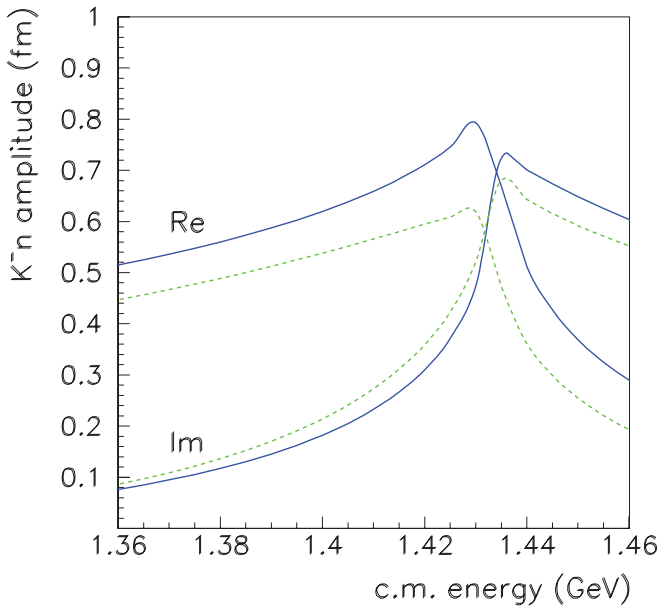

FIG. 4. (Color online) Same as Fig. 3, but for $K^- n$; $N_{K^- n} = 5(6)$ for our model (BNW model).

HADES collaboration results [99] lead to mass spectra different from the somewhat old kaon beam data [92] depicted in Fig. 5, but also from preliminary measurements with photon beams at JLab [101] and SPring-8/LEPS [102]. Final results using electromagnetic probes will hopefully allow checking if the mass spectra depend on the entrance channel, as claimed by the HADES collaboration [99].

Moreover, the experimental project at J-PARC [103] on the in-flight (K^-,n) reaction on deuteron is expected to deepen our understanding of the $(\pi\Sigma)^\circ$ invariant-mass spectra, via the $K^- d \to (\pi\Sigma)^\circ n$ process [104,105].

Finally, to get insights into the quasibound $K^- p$ states, via $\pi\Sigma$ mass spectra, K^- absorption in deuterium [94,96,106], as well as in ^3He and ^4He [5,6,107] have been investigated theoretically. For a recent review on the nature of $\Lambda(1405)$ see Ref. [24].

6. *Summary on two-body interactions*

The main novelty of the present work with respect to our previous investigations [3,4] is the chiral unitary approach to describe $\overline{K}N$ interactions, as presented above.

To facilitate the reading of the paper, we summarize the ingredients for other two-body channels needed to move to the $K^- d$ studies, as reported in detail in Ref. [4]:

(1) *NN interactions*. For the deuteron (d) channel, we used a relativistic separable potential. All the interactions

considered are of rank-1, which allows correctly reproducing the static parameters; namely, the triplet effective range parameters a_t and r_t, the D-state percentage value P_D, the quadrupole moment Q, and the asymptotic ratio $\eta = A_D/A_S$, the $^3S_1$ phase shift, and also the deuteron monopole charge form factor up to about 6 fm^{-1}. In this model the D-state probability is $P_D = 6.7\%$. All details can be found in Ref. [108].

(2) *$\pi N - P_{33}$ and hyperon-proton interactions*. Using the same models as in Ref. [4], we have found that these interactions do not have a significant effect on the K^-d scattering length. We therefore will not bring these partial waves in our discussion.

In conclusion, the obtained $\overline{K}N$ model and handling of the NN two-body channels lead to a reliable enough elementary interactions description to be used in the three-body calculation.

III. K^-d SCATTERING LENGTH

Pioneer work by Toker, Gal, and Eisenberg [109], some three decades ago, initiated theoretical investigations [3,4,47,53,110–113] on the K^-d scattering length, in spite of lack of data, though foreseen in the near future. For recent reviews see Refs. [114,115].

A. Three-body equations for the K^-d system

Here, we summarize the three-body equation formalism for the K^-d system, in which the two-body input described in the previous section will enter. Then we give the expression for the K^-d scattering length.

As the calculations are performed in particle basis, the equations below are given in this basis.

The three-body formalism, where the two-body operators connect two states embodying particles which are different, lead to the following system of coupled equations, written in operator form:

$$X_{a\,b}(s) = Z_{a\,b}(s) + \sum_{c,\,c'} Z_{a\,c}(s) R_{c\,c'}(s)\; X_{c'\,b}(s), \qquad (17)$$

with s the three-body total energy. Here, a, b, c, and c' are the indices which specify the particles involved in the spectator and the interacting pair three-body channels. X_{ab} is the transition amplitude between channels a and b, and Z_{ab} is the corresponding Born term. The two-body operator $R_{c\,c'}$ connects two different two-body states labeled as c and c'.

In the particle basis the particles belonging to the various isospin multiplets do have their physical masses. The number of three-body channels is thus considerably enlarged compared to the case of isospin basis. So, when using our c or s model, the $\overline{K}N$ interactions must include the eight channels coupled to K^-p, namely, K^-p, $\overline{K}^\circ n$, $\pi^-\Sigma^+$, $\pi^+\Sigma^-$, $\pi^\circ\Sigma^\circ$, $\pi^\circ\Lambda$, $\eta\Sigma^\circ$, $\eta\Lambda$, as well as the five channels coupled to K^-n: K^-n, $\pi^-\Sigma^\circ$, $\pi^\circ\Sigma^-$, $\pi^-\Lambda$, $\eta\Sigma^-$.

Now, we specify the values taken by the channel indices in Eq. (17). Taking into account the deuteron and the 13 ($N_{K^-p} + N_{K^-n} = 8 + 5$) two-body inputs in our approach, one must consider the three-body channels in the particle basis as given in Table V, where in the first and fourth lines the *spectator* particles followed (in parentheses) by the associated *pair* are specified.

Starting from the formal equations (17), the final relativistic equations for the rotationally invariant amplitudes are derived [4,116–118]:

$$X^{\mathcal{J}}_{\tau_a\tau_c}(p_a, p_c; s) = Z^{\mathcal{J}}_{\tau_a\tau_c}(p_a, p_c; s) + \sum_{b,\tau_b;b',\tau_{b'}} \int \frac{dp_b\, p_b^2}{2\epsilon_b} Z^{\mathcal{J}}_{\tau_a\tau_b} \times (p_a, p_b; s) R^{c_b=c_{b'}}_{bb'}(\sigma_b) X^{\mathcal{J}}_{\tau_{b'}\tau_c}(p_b, p_c; s), \qquad (18)$$

where σ_b is the invariant energy of the pair in channel b expressed in the three-body center of mass system, $c_a = (J_a, S_a, I_a)$ specifies the conserved quantum numbers of the pair in channel a, and $\tau_a = (c_a, l_a, \Sigma_a)$ specifies the three-body quantum numbers in this channel. Labels c and τ refer to the spin-isospin variables in a given channel. For example, assuming that channel a is composed with particle i as spectator and the pair (jk), we define the following quantities:

(i) $\boldsymbol{s}_i$: spin of particle i,
(ii) $\boldsymbol{S}_i$ $(= \boldsymbol{s}_j + \boldsymbol{s}_k)$, $\boldsymbol{L}_i$, and $\boldsymbol{J}_i$ $(= \boldsymbol{L}_i + \boldsymbol{S}_i)$: spin, orbital angular momentum, and total angular momentum, respectively, of pair (jk),
(iii) $\boldsymbol{\Sigma}_i$ $(= \boldsymbol{s}_i + \boldsymbol{J}_i)$, $\boldsymbol{l}_i$, and $\mathcal{J}$ $(= \boldsymbol{l}_i + \boldsymbol{\Sigma}_i)$: channel spin, orbital angular momentum of i and (jk), and three-body total angular momentum, respectively.

The Born terms matrix in the considered case is a 14×14 matrix. However, only a few terms are nonzero, as explained in what follows:

(i) $Z_p = \langle\, K^-(pn)\,|G_0|\,n(K^-p)\,\rangle$: exchange of the p between the deuteron and the (K^-p) pair,
(ii) $Z_n = \langle\, K^-(pn)\,|G_0|\,p(K^-n)\,\rangle$: exchange of the n between the deuteron and the (K^-n) pair,
(iii) $Z_{K^-} = \langle\, n(K^-p)\,|G_0|\,p(K^-n)\,\rangle$: exchange of the K^- between the (K^-p) and (K^-n) pairs,
(iv) $Z_{\overline{K}^\circ} = \langle\, n(\overline{K}^\circ n)\,|G_0|\,n(\overline{K}^\circ n)\,\rangle$: exchange of the $\overline{K}^\circ$ between the $(\overline{K}^\circ n)$ pairs.

Of course, we must add the corresponding symmetric Born terms, for which the explicit expressions can be found in Ref. [118].

To obtain the rotationally invariant equations, we only have to antisymmetrize the $Z_{\overline{K}^\circ} = \langle\, n(\overline{K}^\circ n)\,|G_0|\,n(\overline{K}^\circ n)\,\rangle$ Born term. This is done as described in Appendix C of Ref. [4].

Concerning the $\overline{K}N$ two-body propagators, they are evaluated as described in Sec. II and Appendix of the present paper, and the d propagator as explained in Ref. [4].

B. Practical calculation

To end this section, we consider the K^-d scattering length, defined as

$$A_{K^-d} = -\lim_{P_K \to 0} \frac{1}{32\pi^2\sqrt{s}} X_{dd}, \qquad (19)$$

TABLE V. The three-body channels in the particle basis. The second line specifies the isospin of the two-body subsystem and the third one the label.

Channel	$K^-(pn)$	$n(K^-p)$	$n(\overline{K}^\circ n)$	$n(\pi^-\Sigma^+)$	$n(\pi^+\Sigma^-)$	$n(\pi^\circ\Sigma^\circ)$	$n(\pi^\circ\Lambda)$
Isospin	0	0	0	0	0	0	0
Label	d	y_1	y_2	α_1	α_2	α_3	α_4
Channel	$n(\eta\Sigma^\circ)$	$n(\eta\Lambda)$	$p(K^-n)$	$p(\pi^-\Sigma^\circ)$	$p(\pi^\circ\Sigma^-)$	$p(\pi^-\Lambda)$	$p(\eta\Sigma^-)$
Isospin	0	0	1	1	1	1	1
Label	μ_1	μ_2	y_3	α_5	α_6	α_7	μ_3

where X_{dd} is the ($\mathcal{J} = 1^-, l = l' = 0$) partial amplitude for K^-d elastic scattering, evaluated at the zero limit for the kaon momentum.

If we retain the contributions of the d+$\overline{K}N$ two-body channels, we have a system of 14 coupled three-body channels (see Table V). After angular momentum reduction, we obtain (in the particle basis) a system of 28 coupled equations for $\mathcal{J} = 1^-$, when including the deuteron d, the eight channels coupled to K^-p, and the five channels coupled to K^-n; see Table VI.

The singularities of the kernel are avoided by using the rotated contour method [119], and, after discretization of the integrals, this system is transformed into a system of linear equations. To solve this system, we use the Padé approximants technique which leads to a convergent solution from the successive iterated terms. In practice, we have used a diagonal [5/5] Padé (constructed with the 11 first iterates), which was found to be sufficient to achieve convergence. Even if the dimension of the matrix to be inverted is somewhat large, this is a sparse matrix because of the limited number of nonzero Born terms, and the Padé approximants method is much less time consuming to solve the linear system than the usual matrix inversion method.

C. Results and discussion

The zero limit for the kaon momentum corresponds to $W \equiv \sqrt{s} = 1431.95$ MeV. As previously emphasized [4], the $\overline{K}N$ scattering length, and in consequence A_{K^-d}, show strong dependence on W, due to proximity of the dominant $\Lambda(1405)$. It is worth to note that the full three-body results are not subject to excessive sensitivities. Actually, the energy dependence in the vicinity of zero limit for the kaon momentum is smeared out due to a loop momentum integral.

Our results for A_{K^-d}, and those from other recent works, are reported in Table VII. We observe that the c and s models for $\overline{K}N$ lead to almost identical values for A_{K^-d}.

A first comment concerns the fact that our present results, both for real and imaginary parts of A_{K^-d}, come out about 12% smaller in magnitude with respect to our 2003 values [4]. These changes are due on the one hand to the improved $\overline{K}N$ model presented in Sec. II, and on the other hand to the since then published SIDDHARTA data [29]. With respect to numerical procedure in $\overline{K}N$ T-matrice calculations, we have carefully checked the convergence of the integral. In our previous model it was ensured by a form factor in the separable form of the interaction, while in the present approach, with no explicit form factor, the amplitudes are tempered by dimensional regularization and converge, though more slowly.

Works by other authors (Table VII) show also the impact of the model used for $\overline{K}N$ interactions and the inclusion or not of the SIDDHARTA data, as discussed below.

Comparing our results with those of BNW, performed before SIDDHARTA data became available, we observe that (i) real parts for model c are identical, while for the s-model BNW values are in between our present and past [4] results. So, the c model is less affected than the s model by the SIDDHARTA data. (ii) The imaginary parts, for both c and s models in BNW are closer to our previous results rather than to those reported in this paper, underlining the significant constraints brought in by the SIDDHARTA data.

All recent results [48,50,120,121] reported in Table VII were obtained considering the SIDDHARTA data, except in Ref. [120].

A new parametrization of the $\overline{K}N \to \pi\Sigma$ potentials was successfully performed by Shevchenko [50] and embodied in the author's [52] coupled-channels Faddeev equations in the Alt-Grassberger-Sandhas form. Results for one- and

TABLE VI. Two-body (L, S, J, T) and three-body (l, Σ, $\mathcal{J}$) quantum numbers in the particle basis, in the case $\mathcal{J} = 1^-$, for $N_{K^-p} = 8$ and $N_{K^-n} = 5$.

Channel	Name	L	S	J	T	Σ	l
$K^-(np)$	d	0,2	1	1	0	1	$\mathcal{J}+1$ $\mathcal{J}-1$
$n(K^-p,\ \overline{K}^\circ n,\ \pi^-\Sigma^+,\ \pi^+\Sigma^-,\ \pi^\circ\Sigma^\circ,\ \pi^\circ\Lambda,\ \eta\Sigma^\circ,\ \eta\Lambda)$	$y_1, y_2, \alpha_1, \alpha_2, \alpha_3, \alpha_4, \mu_1, \mu_2$	0	1/2	1/2	0	1	$\mathcal{J}+1$ $\mathcal{J}-1$
$p(K^-n,\ \pi^-\Sigma^\circ,\ \pi^\circ\Sigma^-\ ,\pi^-\Lambda,\ \eta\Sigma^-)$	$y_3, \alpha_5, \alpha_6, \alpha_7, \mu_3$	0	1/2	1/2	1	1	$\mathcal{J}+1$ $\mathcal{J}-1$

TABLE VII. K^-d scattering length (in fm).

Authors [Ref.]	A_{K^-d}
Present work (c)	$-1.58+i1.37$
Borasoy *et al.* [37] [BNW (c)]	$-1.59+i1.59$
Present work (s)	$-1.57+i1.37$
Borasoy *et al.* [37] [BNW (s)]	$-1.67+i1.52$
Doring-Meissner [48]	$-1.46+i1.08$
Shevchenko [50] (one-pole)	$-1.48+i1.22$
Shevchenko [50] (two-pole)	$-1.51+i1.23$
Revai [120] (one-pole)	$-1.52+i0.98$
Revai [120] (two-pole)	$-1.60+i1.12$
Oset *et al.* [121]	$-1.54+i1.82$
Bahaoui *et al.* [4]	$-1.80+i1.55$

two-pole structures of $\Lambda(1405)$ lead to almost identical values (Table VII) for A_{K^-d}, showing that the scattering length is not sensitive enough to the poles structure of the $\Lambda(1405)$ resonance. Both real and imaginary parts are comparable to our values within less than 10%. Note that in Ref. [50] the NN interactions contain no D state.

Revai [120] using a similar three-body formalism, finds slightly larger differences between one- and two-pole schemes, especially for the imaginary part of the scattering length, which turns out be lower than predictions from all other works quoted in Table VII. These features might be due to the fact that the two-body channels have been investigated using the KEK data rather than the SIDDHARTA results. Actually, Shevchenko has reported such a sensitivity considering SIDDHARTA [50] versus KEK [52] measurements.

Finally, two recent works based on the fixed center approximation (FCA), within a nonrelativistic effective field theory [48] and Faddeev equations [121], lead to discrepancies in real and imaginary parts of about 24% and 44%, respectively. However, a careful study [48] on the accuracy of predicted A_{K^-d} puts forward an "allowed" surface in the [Re(A_{K^-d}), Im(A_{K^-d})] plane. Interestingly, all the results shown in Table VII fall within a somewhat compact subspace of that plane. The forthcoming data from the SIDDHARTA Collaboration [122] will, hopefully, provide sufficient constraints on that physical subspace.

IV. SUMMARY AND CONCLUSIONS

In Sec. II we performed a comprehensive study on the two-body $\overline{K}N$ interactions at low energies via a chiral unitary model including the next-to-leading order terms and the coupled Bethe-Salpeter equations. The emphasis was put on the recent kaonic hydrogen data released by the SIDDHARTA Collaboration [29], which allowed a consistent use of low-energy data to extract the 13 adjustable parameters in our approach and reproduce satisfactorily the fitted data.

Using SU(3) symmetry and the scattering amplitudes for the processes $K^-p \to K^-p, \overline{K}^0n, \Lambda\pi^0, \Sigma^+\pi^-, \Sigma^0\pi^0, \Sigma^-\pi^+, \Lambda\eta, \Sigma^0\eta$, those for the reactions $K^-n \to K^-n, \Lambda\pi^-, \Sigma^0\pi^-, \Sigma^-\pi^0, \Sigma^-\eta$ were also determined, providing the needed complete $\overline{K}N$ inputs to the K^-d system investigations.

Within the two-body studies, we put forward predictions for entities of interest, namely, scattering amplitudes and lengths, as well as the $(\pi\Sigma)^0$ invariant-mass spectra. Results from other authors having used the SIDDHARTA data give comparable results, e.g., for the scattering length $a_{K^-p\to K^-p}$. Data for $(\pi\Sigma)^0$ invariant-mass spectra have never been used to constrain the models, because of poor statistics. Forthcoming data, hopefully accurate enough, using hadronic [95,98,99] or electromagnetic probes [101,102] are expected to significantly improve our knowledge on the $\Lambda(1405) \to (\pi\Sigma)^0$ transitions and hence on the $\overline{K}N$ low-energy interactions. The latter is also of paramount importance in pinning down whether the antikaon is or is not bound in few-body nuclear systems, for which advanced formalisms have been developed [123].

The elementary operators obtained in Sec. II were then used in our three-body equations approach, embodying the relevant NN two-body channel, namely the deuteron, which was described using a relativistic separable potential, with the D-state probability $P_D = 6.7\%$.

Our prediction for the K^-d scattering length is $A_{K^-d} = -1.58 + i\,1.37$. Results from various calculations need to be compared to the forthcoming data from the SIDDHARTA Collaboration [122].

ACKNOWLEDGMENTS

T.M. would like to acknowledge several pleasant visits extended to him at the Thomas Jefferson National Accelerator Facility. He also would like to thank Bugra Borasoy, Wolfram Weise, and Antonio Oller for clarifications regarding their works. Thanks are also extended to Tony Thomas for reminding him of the earlier SU(3) *cloudy bag* approach to the $\overline{K}N - \pi\Sigma$ channels. The work of K.T. was supported by the University of Adelaide and the Australian Research Council through Grant No. FL0992247 (AWT). K.T. also would like to acknowledge the International Institute of Physics, Federal University of Rio Grande do Norte, Natal, Brazil, for warm hospitality during which part of this work was carried out.

APPENDIX: TWO-BODY $\overline{K}N$ AMPLITUDES

Because we have closely followed the definition and convention used in BNW [37], not much may be needed to repeat the description of the quantities in the $\overline{K}N$ equations. So, we will simply give some supplementary information.

1. Relation to our previous notations

In case the reader may find it useful, the quantities we adopted in our 2003 work [4] denoted as *LYS* ≡ *Lyon-Saclay* are related to those in BNW as

$$V_{\rm LYS} = -4\pi\, V_{\rm BNW}, \tag{A1}$$

$$T_{\rm LYS} = -4\pi\, T_{\rm BNW}, \tag{A2}$$

$$G_{\rm LYS} = \frac{1}{4\pi} G_{\rm BNW}, \tag{A3}$$

and the corresponding scattering amplitude reads

$$f_{\rm LYS} = -\frac{1}{32\pi^2\sqrt{s}} T_{\rm LYS}, \tag{A4}$$

where s is the Mandelstam variable of the channel.

2. Two-body meson-baryon scalar loop

In BNW this function is explicitly given in their Eq. (11). We also used the same subtraction scale value, $\mu = 1.0$ GeV, and m and M are the generic meson and baryon masses, respectively. For our practical implementation, we have used a somewhat different form of the propagator which is completely equivalent to the form in BNW. We also checked the equivalence of our form with the one used in Ref. [41]. For convenience, we split G into three parts:

$$G_{\rm BNW}(s) = G_1 + G_2 + G_3, \tag{A5}$$

where the constant term is

$$G_1 = a(\mu) + \frac{1}{32\pi^2}\left[\ln\left(\frac{m^2}{\mu^2}\right) + \ln\left(\frac{M^2}{\mu^2}\right) - 2\right], \tag{A6}$$

with $a(\mu)$ the subtraction constant. Then

$$G_2 = \frac{1}{32\pi^2 s}(m^2 - M^2)\ln\left(\frac{m^2}{M^2}\right), \tag{A7}$$

and

$$G_3 = \frac{1}{32\pi^2 s} 4mM\sqrt{z^2-1}\ln(-z-\sqrt{z^2-1}), \tag{A8}$$

where

$$z = \frac{s - M^2 - m^2}{2mM}. \tag{A9}$$

It might be useful to remember that at the threshold, $s = (M+m)^2$, $z = 1$. Also $z = -1$ at $s = (M-m)^2$. Then it can be shown that G is analytic in the whole complex s plane with an unitarity cut on the positive real axis starting from the threshold: $s = (M+m)^2$. An apparent singularity at $s = 0$ in the above expression, which might derive from the kinematics at origin, must be absent. Explicitly we looked at the small $|s|$ behavior and found that

$$G_2 + G_3 \approx \frac{1}{16\pi^2}\left[1 - \frac{M^2+m^2}{2(M^2-m^2)}\ln\left(\frac{m^2}{M^2}\right)\right] \tag{A10}$$

$$- \frac{1}{32\pi^2(M^2-m^2)^2} \times \left[(M^2+m^2) + \frac{2(Mm)^2}{(M^2-m^2)}\ln\left(\frac{m^2}{M^2}\right)\right]s. \tag{A11}$$

So, in numerical calculation in the three-body code where the vanishing value of s may be encountered, those two contributions need to be calculated together to avoid possible spurious divergences.

[1] N. Kaiser, P. B. Siegel, and W. Weise, Nucl. Phys. A **594**, 325 (1995).
[2] E. Oset and A. Ramos, Nucl. Phys. A **635**, 99 (1998).
[3] A. Bahaoui, C. Fayard, T. Mizutani, and B. Saghai, Phys. Rev. C **66**, 057001 (2002).
[4] A. Bahaoui, C. Fayard, T. Mizutani, and B. Saghai, Phys. Rev. C **68**, 064001 (2003).
[5] T. Yamazaki and Y. Akaishi, Phys. Lett. B **535**, 70 (2002).
[6] Y. Akaishi and T. Yamazaki, Phys. Rev. C **65**, 044005 (2002).
[7] T. Yamazaki and Y. Akaishi, Phys. Rev. C **76**, 045201 (2007).
[8] N. V. Shevchenko, A. Gal, and J. Mares, Phys. Rev. Lett. **98**, 082301 (2007).
[9] N. V. Shevchenko, A. Gal, J. Mares, and J. Revai, Phys. Rev. C **76**, 044004 (2007).
[10] Y. Ikeda and T. Sato, Phys. Rev. C **76**, 035203 (2007).
[11] Y. Ikeda and T. Sato, Phys. Rev. C **79**, 035201 (2009).
[12] A. Dote and W. Weise, Prog. Theor. Phys. Suppl. **168**, 593 (2007).
[13] A. Dote, T. Hyodo, and W. Weise, Nucl. Phys. A **804**, 197 (2008).
[14] A. Dote, T. Hyodo, and W. Weise, Phys. Rev. C **79**, 014003 (2009).
[15] Y. Ikeda, H. Kamano, and T. Sato, Prog. Theor. Phys. **124**, 533 (2010).
[16] Y. Ikeda, T. Hyodo, and W. Weise, Phys. Lett. B **706**, 63 (2011).
[17] Y. Ikeda, T. Hyodo, and W. Weise, Nucl. Phys. A **881**, 98 (2012).
[18] M. Bayar, J. Yamagata-Sekihara, and E. Oset, Phys. Rev. C **84**, 015209 (2011).
[19] E. Oset, D. Jido, T. Sekihara, M. Bayar, and J. Yamagata-Sekihara, arXiv:1108.3928.
[20] M. Bayar and E. Oset, arXiv:1207.1661.
[21] T. Sekihara, J. Yamagata-Sekihara, D. Jido, and Y. Kanada-En'yo, Phys. Rev. C **86**, 065205 (2012).
[22] D. Gazda and J. Mares, Nucl. Phys. A **881**, 159 (2012).
[23] M. Mai and U. G. Meissner, Nucl. Phys. A **900**, 51 (2013).
[24] T. Hyodo and D. Jido, Prog. Part. Nucl. Phys. **67**, 55 (2012).
[25] A. D. Martin, Nucl. Phys. B **179**, 33 (1981).
[26] M. Iwasaki *et al.*, Phys. Rev. Lett. **78**, 3067 (1997).
[27] T. M. Ito *et al.*, Phys. Rev. C **58**, 2366 (1998).
[28] G. Beer *et al.* (DEAR Collaboration), Phys. Rev. Lett. **94**, 212302 (2005).
[29] M. Bazzi *et al.* (SIDDHARTA Collaboration), Phys. Lett. B **704**, 113 (2011).
[30] J. A. Oller and U. G. Meissner, Phys. Lett. B **500**, 263 (2001).
[31] J. A. Oller, E. Oset, and A. Ramos, Prog. Part. Nucl. Phys. **45**, 157 (2000).
[32] M. F. M. Lutz and E. E. Kolomeitsev, Nucl. Phys. A **700**, 193 (2002).
[33] E. Oset, A. Ramos, and C. Bennhold, Phys. Lett. B **527**, 99 (2002); **530**, 260 (2002).
[34] T. Hyodo, S. I. Nam, D. Jido, and A. Hosaka, Phys. Rev. C **68**, 018201 (2003).
[35] D. Jido, J. A. Oller, E. Oset, A. Ramos, and U. G. Meissner, Nucl. Phys. A **725**, 181 (2003).

[36] B. Borasoy, R. Nissler, and W. Weise, Phys. Rev. Lett. **94**, 213401 (2005).
[37] B. Borasoy, R. Nissler, and W. Weise, Eur. Phys. J. A **25**, 79 (2005).
[38] B. Borasoy, U. G. Meissner, and R. Nissler, Phys. Rev. C **74**, 055201 (2006).
[39] J. A. Oller, J. Prades, and M. Verbeni, Phys. Rev. Lett. **95**, 172502 (2005).
[40] J. A. Oller, J. Prades, and M. Verbeni, Phys. Rev. Lett. **96**, 199202 (2006).
[41] J. A. Oller, Eur. Phys. J. A **28**, 63 (2006).
[42] A. Cieply and J. Smejkal, Eur. Phys. J. A **34**, 237 (2007).
[43] A. Cieply and J. Smejkal, Eur. Phys. J. A **43**, 191 (2010).
[44] S. S. Kamalov, E. Oset, and A. Ramos, Nucl. Phys. A **690**, 494 (2001).
[45] A. Sibirtsev, M. Buescher, V. Y. Grishina, C. Hanhart, L. A. Kondratyuk, S. Krewald, and U. G. Meissner, Phys. Lett. B **601**, 132 (2004).
[46] V. Kleber *et al.*, Phys. Rev. Lett. **91**, 172304 (2003).
[47] U. G. Meissner, U. Raha, and A. Rusetsky, Eur. Phys. J. C **47**, 473 (2006).
[48] M. Doring and U. G. Meissner, Phys. Lett. B **704**, 663 (2011).
[49] V. Baru, E. Epelbaum, and A. Rusetsky, Eur. Phys. J. A **42**, 111 (2009).
[50] N. V. Shevchenko, Nucl. Phys. A **890-891**, 50 (2012).
[51] A. Bahaoui, C. Fayard, G. H. Lamot, and T. Mizutani, Nucl. Phys. A **508**, 335C (1990).
[52] N. V. Shevchenko, Phys. Rev. C **85**, 034001 (2012).
[53] M. Faber, M. P. Faifman, A. N. Ivanov, J. Marton, M. Pitschmann, and N. I. Troitskaya, Phys. Rev. C **84**, 064314 (2011).
[54] F. E. Close and R. G. Roberts, Phys. Lett. B **316**, 165 (1993).
[55] P. C. Bruns, M. Mai, and U. G. Meissner, Phys. Lett. B **697**, 254 (2011).
[56] K. Nakamura *et al.* (Particle Data Group), J. Phys. G **37**, 075021 (2010).
[57] G. S. Abraham and B. Sechi-Zorn, Phys. Rev. **139**, 454 (1965).
[58] M. Csejthey-Barth *et al.*, Phys. Lett. **16**, 89 (1965).
[59] M. Sakitt, T. B. Day, R. G. Glasser, N. Seeman, J. H. Friedman, W. E. Humphrey, and R. R. Ross, Phys. Rev. **139**, B719 (1965).
[60] W. Kittel, G. Otter, and I. Wacek, Phys. Lett. **21**, 349 (1966).
[61] J. K. Kim, Phys. Rev. Lett. **19**, 1074 (1967).
[62] T. S. Mast, M. Alston-Garnjost, R. O. Bangerter, A. S. Barbaro-Galtieri, F. T. Solmitz, and R. D. Tripp, Phys. Rev. D **11**, 3078 (1975).
[63] T. S. Mast, M. Alston-Garnjost, R. O. Bangerter, A. S. Barbaro-Galtieri, F. T. Solmitz, and R. D. Tripp, Phys. Rev. D **14**, 13 (1976).
[64] R. O. Bangerter, M. Alston-Garnjost, A. Barbaro-Galtieri, T. S. Mast, F. T. Solmitz, and R. D. Tripp, Phys. Rev. D **23**, 1484 (1981).
[65] J. Ciborowski *et al.*, J. Phys. G **8**, 13 (1982).
[66] D. Evans, J. V. Major, E. Rondio, J. A. Zakrzewski, J. E. Conboy, D. J. Miller, and T. Tymieniecka, J. Phys. G **9**, 885 (1983).
[67] P. B. Siegel and B. Saghai, Phys. Rev. C **52**, 392 (1995).
[68] W. E. Humphrey and R. R. Ross, Phys. Rev. **127**, 1305 (1962).
[69] D. N. Tovee *et al.*, Nucl. Phys. B **33**, 493 (1971).
[70] R. J. Nowak *et al.*, Nucl. Phys. B **139**, 61 (1978).
[71] J. Gasser, H. Leutwyler, and M. E. Sainio, Phys. Lett. B **253**, 252 (1991).
[72] T. Inoue, V. E. Lyubovitskij, T. Gutsche, and A. Faessler, Phys. Rev. C **69**, 035207 (2004).
[73] J. Martin Camalich, L. S. Geng, and M. J. Vicente Vacas, Phys. Rev. D **82**, 074504 (2010).
[74] G. E. Hite, W. B. Kaufmann, and R. J. Jacob, Phys. Rev. C **71**, 065201 (2005).
[75] R. A. Arndt, W. J. Briscoe, I. I. Strakovsky, R. L. Workman, and M. M. Pavan, Phys. Rev. C **69**, 035213 (2004).
[76] S. Durr *et al.*, Phys. Rev. D **85**, 014509 (2012).
[77] G. S. Bali *et al.* (QCDSF Collaboration), Phys. Rev. D **85**, 054502 (2012).
[78] P. E. Shanahan, A. W. Thomas, and R. D. Young, arXiv:1205.5365.
[79] C. S. An, B. Saghai, S. G. Yuan, and J. He, Phys. Rev. C **81**, 045203 (2010).
[80] H. Dahiya and N. Sharma, AIP Conf. Proc. **1388**, 439 (2011).
[81] C. S. An and B. Saghai, PoS **QNP2012**, 077 (2012).
[82] A. Starostin *et al.* (Crystal Ball Collaboration), Phys. Rev. C **64**, 055205 (2001).
[83] B.-C. Liu and J.-J. Xie, Phys. Rev. C **85**, 038201 (2012).
[84] D. A. Sharov, V. L. Korotkikh, and D. E. Lanskoy, Eur. Phys. J. A **47**, 109 (2011).
[85] R. Shyam, O. Scholten, and A. W. Thomas, Phys. Rev. C **84**, 042201 (2011).
[86] A. Cieply and J. Smejkal, Nucl. Phys. A **881**, 115 (2012).
[87] V. Krejcirik, Phys. Rev. C **86**, 024003 (2012).
[88] W. Weise, Nucl. Phys. A **835**, 51 (2010).
[89] U. G. Meissner, U. Raha, and A. Rusetsky, Eur. Phys. J. C **35**, 349 (2004).
[90] T. Hyodo and W. Weise, Phys. Rev. C **77**, 035204 (2008).
[91] J. Revai and N. V. Shevchenko, Phys. Rev. C **79**, 035202 (2009).
[92] R. J. Hemingway, Nucl. Phys. B **253**, 742 (1985).
[93] J. C. Nacher, E. Oset, H. Toki, and A. Ramos, Phys. Lett. B **455**, 55 (1999).
[94] D. Jido, E. Oset, and T. Sekihara, Eur. Phys. J. A **47**, 42 (2011).
[95] I. Zychor *et al.*, Phys. Lett. B **660**, 167 (2008).
[96] J. Esmaili, Y. Akaishi, and T. Yamazaki, Phys. Rev. C **83**, 055207 (2011).
[97] L. S. Geng and E. Oset, Eur. Phys. J. A **34**, 405 (2007).
[98] G. Agakishiev, A. Balanda, D. Belver, A. Belyaev, J. C. Berger-Chen, A. Blanco, M. Boehmer, J. L. Boyard *et al.*, Nucl. Phys. A **881**, 178 (2012).
[99] G. Agakishiev, A. Balanda, D. Belver, A. V. Belyaev, J. C. Berger-Chen, A. Blanco, M. Bohmer, J. L. Boyard *et al.*, arXiv:1208.0205.
[100] E. Epple and L. Fabbietti (HADES Collaboration), Hyperfine Interact. **210**, 45 (2012).
[101] K. Moriya and R. Schumacher (CLAS Collaboration), AIP Conf. Proc. **1432**, 371 (2012).
[102] J. K. Ahn (LEPS Collaboration), Nucl. Phys. A **835**, 329 (2010).
[103] S. Enomoto *et al.*, AIP Conf. Proc. **1388**, 599 (2011).
[104] K. Miyagawa and J. Haidenbauer, Phys. Rev. C **85**, 065201 (2012).
[105] D. Jido, E. Oset, and T. Sekihara, arXiv:1207.5350 [nucl-th].
[106] V. Kopeliovich and I. Potashnikova, Phys. Rev. C **83**, 064302 (2011).
[107] J. Esmaili, Y. Akaishi, and T. Yamazaki, Phys. Lett. B **686**, 23 (2010).
[108] N. Giraud, C. Fayard, and G. H. Lamot, Phys. Rev. C **21**, 1959 (1980).

[109] G. Toker, A. Gal, and J. M. Eisenberg, Nucl. Phys. A **362**, 405 (1981).
[110] R. C. Barrett and A. Deloff, Phys. Rev. C **60**, 025201 (1999).
[111] A. Deloff, Phys. Rev. C **61**, 024004 (2000).
[112] V. Y. Grishina, L. A. Kondratyuk, M. Buescher, and W. Cassing, Eur. Phys. J. A **21**, 507 (2004).
[113] A. N. Ivanov *et al.*, Eur. Phys. J. A **23**, 79 (2005).
[114] A. Gal, Int. J. Mod. Phys. A **22**, 226 (2007).
[115] J. Gasser, V. E. Lyubovitskij, and A. Rusetsky, Phys. Rept. **456**, 167 (2008).
[116] R. Aaron, R. D. Amado, and J. E. Young, Phys. Rev. **174**, 2022 (1968).
[117] A. S. Rinat and A. W. Thomas, Nucl. Phys. A **282**, 365 (1977).
[118] A. Bahaoui, Ph.D. thesis, Université Claude Bernard Lyon I, 1990.
[119] J. H. Hetherington and L. H. Schick, Phys. Rev. **156**, 1647 (1967).
[120] J. Revai, arXiv:1203.1813.
[121] E. Oset, D. Jido, T. Sekihara, A. M. Torres, K. P. Khemchandani, M. Bayar, and J. Yamagata-Sekihara, Nucl. Phys. A **881**, 127 (2012).
[122] S. Okada *et al.* (SIDDHARTA Collaboration), PoS **FACESQCD**, 047 (2010).
[123] T. Hyodo, arXiv:1209.6208.